

SHIFT AND ROTATION INVARIANT IRIS FEATURE EXTRACTION BASED ON NON-SUBSAMPLED CONTOURLET TRANSFORM AND GLCM

Sirvan Khalighi¹, Parisa Tirdad², Fatemeh Pak² and Urbano Nunes¹

¹University of Coimbra, 3030-790 Coimbra, Portugal, and Institute for Systems and Robotics (ISR-UC)

²Department of Electrical and Computer Engineering, AZAD University of Qazvin, Qazvin, Iran

Keywords: Gray Level Co-occurrence Matrix, Iris Recognition, Non-Subsampled Contourlet Transform, SVM.

Abstract: A new feature extraction method for iris recognition in non-subsampled contourlet transform (NSCT) domain is proposed. To extract the features a two-level NSCT, which is a shift-invariant transform, and a rotation-invariant gray level co-occurrence matrix (GLCM) with 3 different orientations are applied on both spatial image and NSCT frequency subbands. The extracted feature set is transformed and normalized to reduce the effect of extreme values in the feature matrix. A set of significant features are selected by using the minimal redundancy and maximal relevance (mRMR) algorithm. Finally the selected feature set is classified using support vector machines (SVMs). The classification results using leave one out cross-validation (LOOCV) on the CASIA iris database, Ver.1 and Ver.4 show that the proposed method performs at the state-of-the art in the field of iris recognition.

1 INTRODUCTION

Iris recognition is regarded as one of the most reliable and accurate biometric identification technologies because of the unique, aging invariant and non-invasive characteristics of iris. This resulted in development of a large number of automatic iris recognition algorithms. Daugman (Daugman, 1993) first introduced a prototype system for automatic iris recognition based on multi-scale Gabor wavelets and extracted the phase information of iris textures. Wildes (Wildes, 1997) applied a gradient-based binary edge map and the Hough transform to detect the iris and pupil boundaries. In (Roy *et al.*, 2011), a wavelet transform was applied to extract the textural features and a genetic algorithm was employed to select the subset of informative features.

Even though, the wavelet transform is popular, powerful and familiar among the iris processing techniques, it has its own limitations in capturing directional information in images such as smooth contours and the directional edges. This problem is addressed by Contourlet Transform (CT) (Do and Vetterli, 2001). In addition to multi-scale and time-frequency localization properties of wavelets, CT offers directionality and anisotropy. A 4-level CT method for iris feature extraction was described in

(Li *et al.*, 2010), in which normalized images are partitioned into multi-scale and multi-directional subbands. The normalized energy of subbands are calculated as features to train a support vector machine (SVM) classifier. Due to downsampling and upsampling, the CT lacks shift-invariance. To overcome this limiting factor, Cunha *et al.* (Cunha *et al.*, 2006) proposed a shift-invariant version of CT designated non-subsampled contourlet transform (NSCT).

In this paper a new scale, shift and rotation invariant feature extraction method for iris recognition in NSCT domain is proposed. After normalizing the selected regions of interest, some textural features are extracted from the gray level co-occurrence matrix (GLCM) of both spatial image and frequency subbands which resulted from NSCT decomposition. To improve the recognition rate, the extracted features are transformed and normalized, then fed into the minimal redundancy and maximal relevance (mRMR) feature selection process. Finally the selected feature set is classified using SVMs.

2 PROPOSED APPROACH

The proposed iris recognition system includes four

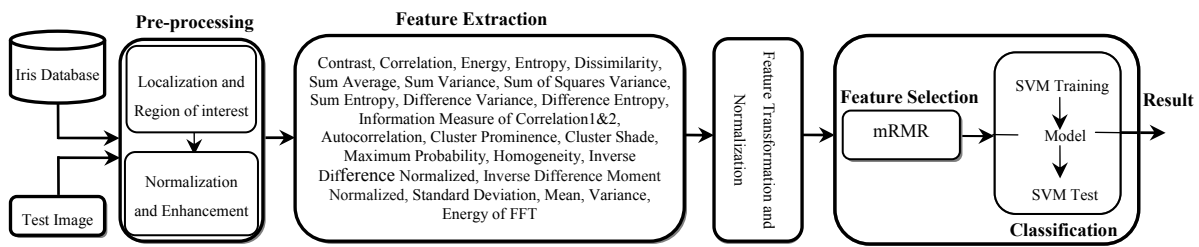


Figure 1: Overall System Architecture.

major phases: a) iris preprocessing, b) feature extraction, c) feature transformation and normalization, and d) feature selection and classification. Figure 1 shows the architecture of the system.

2.1 Iris Pre-processing

For the purpose of iris recognition some irrelevant parts such as eyelid, sclera, eyelashes and pupil should be removed. In addition, even for the iris of the same eye, the size may vary depending on camera-to-eye distance as well as light brightness. Therefore, the original image needs to be pre-processed to localize, normalize and enhance the iris regions, and reduce the influence of the mentioned factors.

Localization and regions of interest selection: To locate the inner (iris/pupil) and the outer (iris/sclera) boundaries, the following steps should be performed:

1) Reflection removal: Specular reflections (light spots in the eye image) can cause some problems in the localization process. To remove the reflections, the eye image is binarized (using a threshold = 190). The binarized eye image is then dilated to consider all possible affected regions. Then the resulted mask is complemented and applied to the eye image for marking the reflections spots. Finally, the detected specular reflections are “inpainted” (Shah and Ross, 2009) using the 8 surrounding neighbours.

2) Pupillary boundary detection: To detect the pupillary boundary, the eye image is first binarized using a threshold value, $M+25$ (Shah and Ross, 2009) where M is the minimum fixed value of the inpainted image. In addition to the pupil, other dark regions of the eye image such as eyelashes fall below this threshold value. In order to eliminate the regions corresponded with the eyelashes, a 2-D median filter with a 10×10 convolution mask is applied on the binary image. This reduces the

number of candidate regions detected as a consequence of thresholding (Shah and Ross, 2009). The remaining regions in the median-filtered binary image are labelled and the region with the largest area and the smallest eccentricity is determined as the pupil region. Finally, the pupil radius and centroid are calculated by (1) and (2) respectively:

$$pupilRadius = (\sqrt{4 \times A / \pi}) / 2 \quad (1)$$

$$(C_x, C_y) = (\int x dA / A, \int y dA / A) \quad (2)$$

where (C_x, C_y) denote the center coordinates of the pupil and A is the area of the pupil.

3) Limbic boundary detection: Before locating the outer boundary, gamma threshold (Masek *et al.*, 2003) is adjusted to the iris edge map (extracted by Canny edge detector) to enhance the iris contrast. Then the weak edge pixels are set to zero using non-maxima suppression; thus only the dominant edges are extracted. Finally, the hysteresis thresholding is applied to the image. Having the pupil center coordinates, the radius and centre coordinates of the iris boundary can be deduced using circular Hough transform.

To disregard the iris regions occluded by the eyelid and eyelashes and to avoid loss of discriminative features, four regions of interest (ROI) are selected:

I) right side of the iris circle, a sector between angles $-\pi/4$ and $\pi/4$ with a radius equal to iris radius (Figure 2 (a)). II) left side of the iris circle, a sector between angles $4\pi/5$ and $4\pi/3$ with a radius equal to iris radius (Figure 2 (a)). III) bottom side of the iris circle, a sector between angles $4\pi/3$ and $-\pi/4$ with a radius of $1/2$ of the iris radius (Figure 2 (b)). IV) a disk around the pupil with a radius of $1/3$ of the iris radius to cover the pupillary area (Figure 2 (c)).

Normalization and enhancement: To compensate several external factors such as illumination variations and imaging distance, the partial iris images are normalized using “Daugman Rubber Sheet” model (Daugman, 1993).

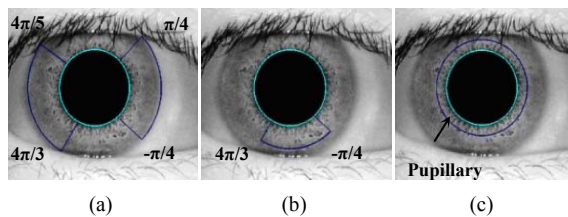


Figure 2: Selected regions for normalization.

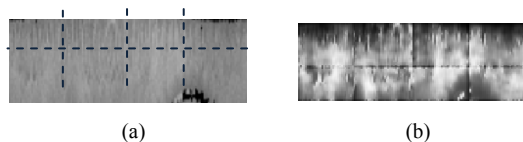


Figure 3: (a) Tiled normalized image. (b) Enhanced iris image by histogram equalization and Wiener filtering.

Since the original iris image has low contrast and may have non-uniform illumination caused by the position of the light sources, some enhancements need to be applied. The histogram equalization is used to enhance the normalized iris images. The enhancement involves tessellating the normalized iris into 32×32 tiles (Figure 3(a)) and subjecting each tile to histogram equalization. Then for noise-removal, the Wiener filter is applied to each tile (Figure 3(b)).

2.2 Feature Extraction

A reliable iris recognition system should extract features that are invariant to scaling, shift and rotation. The scale invariance is obtained by unwrapping the selected iris regions into four fixed size rectangles. To achieve shift invariance, the enhanced images are transformed into the frequency domain using the NSCT which is a shift-invariant transform and can capture the geometry of the iris texture. Finally, the GLCM is calculated on both spatial image and NSCT frequency subbands. The proposed method is described as follows.

Non-subsampled contourlet transform: In contourlet transform, the Laplacian Pyramid (LP) is first used to capture point discontinuities, and then followed by a Directional Filter Bank (DFB) to link point discontinuities into linear structures (Po and Do, 2006). The overall result is an image expansion using basic elements like contour segments, and thus called contourlet transform, which is implemented by a Pyramidal Directional Filter Bank (PDFB) (Do and Vetterli, 2001). The LP decomposition at each level generates a down sampled low pass version of the original image, and the difference between the

original image and the prediction results in a bandpass image. Due to downsampling and upsampling presented in both LP and DFB, contourlet transform is not shift-invariant. The NSCT is built upon nonsubsampling pyramids and nonsubsampling directional filter bank (NSDFB); thus, it is a fully shift-invariant, multi-scale, and multi-direction image decomposition that has a fast implementation (Cunha *et al.*, 2006).

Primary features: The enhanced iris image is decomposed into 6 directions using NSDFB at 2 different scales. Afterward some textural features are extracted from the spatial iris image and all NSCT frequency subbands. Textural features mentioned in Figure 1 are computed on the basis of statistical distribution of pixels' intensity at a given position relative to others in a matrix of pixels called GLCM (Haralick *et al.*, 1973). Since the GLCM is computed for different orientations, the rotation of the iris can be captured by one of the matrices. Feature extraction based on GLCM is a second-order statistic that can be employed to analyze an image as a texture. Although GLCM captures properties of a texture, it cannot be directly used for further analysis, such as the comparison of two textures; thus numeric features which contain significant information about the textural characteristics are obtained from the GLCM in three different directions (Haralick *et al.*, 1973), (Soh *et al.*, 1999) and (Clausi *et al.*, 2002).

2.3 Feature Transformation and Normalization

The extracted features are transformed and normalized in order to reduce the influence of extreme values. The transformation methods applied to each feature are described in (Becq *et al.*, 2005). After a thorough experimental evaluation of each transform operator over extracted features, it was empirically verified that the best classification results were attained with the transform $\mathbf{X} = 1/\sqrt{\mathbf{Y}}$, where \mathbf{Y} denotes the feature matrix, and $\mathbf{X} = \{x_{ij}; i = 1, 2, \dots, N \text{ and } j = 1, 2, \dots, M\}$ (where N and M denote the number of subjects and features respectively) is the transformed feature matrix. Thereby this transform was adopted in the overall iris recognition system. To avoid features in greater numeric ranges dominating those in smaller numeric ranges, each feature of the transformed matrix \mathbf{X} is independently normalized to the (0, 1) range by applying

$$\bar{x}_{ij} = x_{ij} / (\max(x_j) - \min(x_j)) \quad (3)$$

where x_j is a vector of each independent feature (Aksoy *et al.*, 2001).

2.4 Feature Selection and Classification

Larger numbers of high-dimensional feature vectors make the classification process more complex and less reliable due to features redundancy. To reduce these effects the mRMR feature selector is used (Peng *et al.*, 2005).

Support vector machines (SVMs) (Burges, 1998) are adopted as classifier in this study, given that neural networks and other classifiers cannot show reliable classification results in too noisy data.

3 EXPERIMENTAL RESULTS

The performance of the proposed algorithm was assessed using CASIA iris image databases Ver.1 and Ver.4-Lamp (CASIA Iris Image Database). CASIA Ver.1 contains a total of 756 grayscale iris images, from 108 subjects, captured in two sessions with at least one month interval. CASIA Ver.4-Lamp was collected using a hand-held iris sensor in one session. It contains 16213 grayscale iris images from 411 subjects. CASIA-Ver. 4-Lamp is suitable for studying problems of non-linear iris normalization and robust iris feature representation because of elastic deformation of iris texture due to pupil expansion and contraction under different illumination conditions.

In our experiments, a two-level NSCT decomposition was adopted with 2 and 4 directions for each pyramidal level respectively. Three GLCMs were calculated on all NSCT frequency subbands and the spatial image both in 0° , 90° and 135° . The normalized iris images were decomposed by the NSPDFB. We have used “pyrex” and “pkva” as NSLP and NSDFB filter in NSPDFB decomposition (Non-subsampled Contourlet Toolbox ver.1.0.0) given their good performance. SVM-KM toolbox (SVM and Kernel Method Toolbox) with Gaussian kernel was used in the classification phase. The Gaussian kernel degree and C parameters were set to 6 and 100 respectively as suggested by the best empirical results. Experiments were carried out over 2000 images of 200 randomly selected classes, with 10 images per class and 756 images of 108 classes for CASIA Ver.4 and Ver.1 respectively.

To estimate the accuracy of classification, leave one out cross-validation (LOOCV) was used.

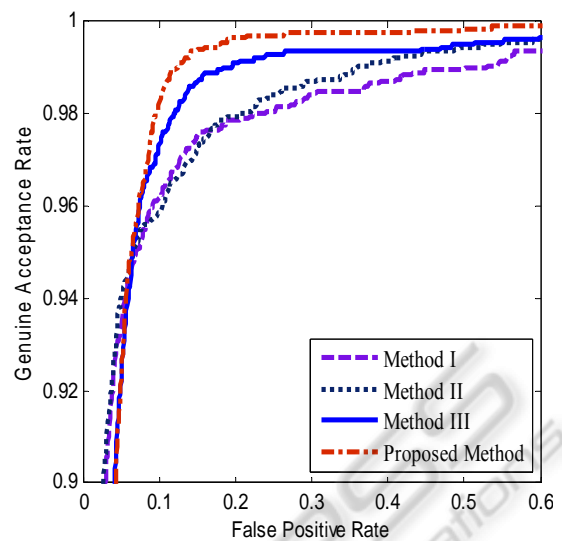


Figure 4: Comparison of selecting different iris ROI in the localization process over the CASIA Ver.4. The parameters of method I are $\Theta = (0, 2\pi)$, $r = \text{IrisR}$, method II $\Theta = (0, 2\pi)$, $r = 1/3 \times \text{IrisR}$ and method III are $\Theta_{\text{Left}} = (3\pi/4, 5\pi/4)$, $\Theta_{\text{Right}} = (-\pi/4, \pi/4)$, $r = \text{IrisR}$.

Receiver operating characteristics (ROC) in Figure 4 show the comparison of different iris localization approaches on the Ver.4. Each curve is denoted by symbols r, Θ which represent normalized polar coordinates. $\Theta = (0, 2\pi)$, $r = \text{IrisR}$ refers to a disk around the iris with iris radius, which covers the whole iris region. $\Theta = (0, 2\pi)$, $r = 1/3 \times \text{IrisR}$ refers to a disk around the iris with 1/3 iris radius, similar to Figure 2 (c). $\Theta_{\text{Left}} = (3\pi/4, 5\pi/4)$, $\Theta_{\text{Right}} = (-\pi/4, \pi/4)$, $r = \text{IrisR}$ refers to a state similar to Figure 2 (a). The results illustrate the superior performance of the proposed approach over the other mentioned methods in Figure 4.

From the feature extraction process, a total of 2048 features for each sample resulted. The transformed and normalized feature matrix was fed into the feature selection method. The number of selected features based on the mRMR results, was set to 357 because it provided the best mean accuracy in a grid search. The most effective features were correlation and homogeneity and the least significant was maximum probability feature in the extracted group (Figure 1). From each ROI, the following numbers of features were selected: 68, 70, 125, 94 which correspond to Figure 2 (a) left, (a) right, (b) and (c) respectively. These results demonstrate that the region between $(4\pi/3, -\pi/4)$ with 1/2 of iris radius contains more relevant features than other regions.

Figure 5 shows the comparison of the proposed feature extraction method using NSCT, contourlet

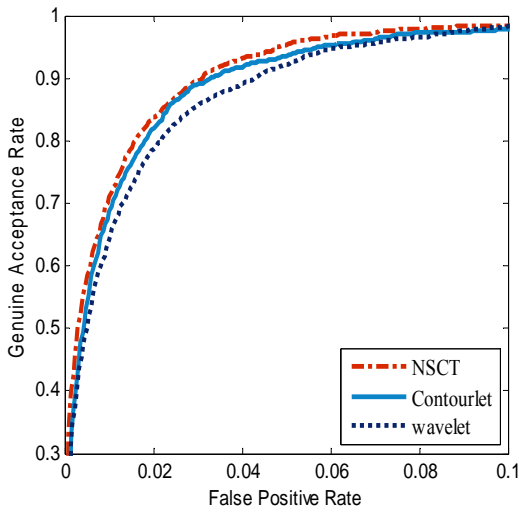


Figure 5: Performance of different feature extraction methods over the CASIA Ver.4.

and wavelet transforms. This diagram shows the highest accuracy obtained by NSCT due to its redundant structure.

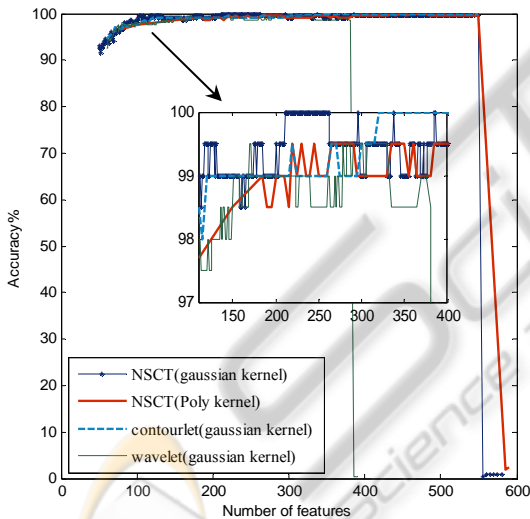


Figure 6: Comparison of classification accuracy for different frequency transformation with different numbers of features over the CASIA Ver.4.

Maximum classification accuracies of NSCT with two different kernels, contourlet and wavelet transforms with different number of features, are shown in Figure 6. For the wavelet transform the best mean accuracy of 93.40% was obtained for 322 features; however this accuracy is lower than the case of using NSCT. For the contourlet transform the best mean accuracy of 96.55% was attained for 490 features, which in comparison with NSCT has a

Table 1: Performance comparison of some popular algorithms on CASIA database Ver. 1.

Methodology	Feature Extraction methods	Accuracy Rate %
Daugman (Daugman, 1993)	Gabor wavelets	100
Qi M. <i>et al.</i> (Qi M. <i>et al.</i> , 2008)	Gabor filter	99.92
Chen <i>et al.</i> (Chen <i>et al.</i> , 2009)	1-D circular profile	99.35
Poursaberi <i>et al.</i> (Poursaberi <i>et al.</i> , 2007)	wavelet Daubechies2	99.31
Our approach without LOOCV	NSCT and GLCM	100
Our approach by LOOCV (mean accuracy)	NSCT and GLCM	98.29

higher number of features. This diagram corroborates the high performance of our approach over the CASIA Ver.4 with the average and maximum accuracies of 96.55% and 100%, respectively. Furthermore, the comparison results of the classification accuracy over the CASIA Ver.1 are as follow. The best mean accuracy of 91.40% with 185 features and 97.35% with 565 features were achieved for the wavelet and contourlet transforms, respectively. The best mean accuracy of 98.29% was achieved with the NSCT using 424 features.

Considering that there isn't any reported result based on CASIA Ver. 4 lamp, the proposed method was compared with state of the art methods, just with CASIA Ver. 1. Table 1 shows the comparison results of the proposed method with the others. Some accuracy results are higher than our mean accuracy, however we highlight that our reported results were obtained using the LOOCV method in the testing process.

4 CONCLUSIONS

A new feature extraction method for iris recognition based on NSCT was presented. The described technique has some advantages over other techniques. First, this method selects four ROIs to make use of the most significant information in the iris texture. Second, the extracted features are invariant to scaling, shift and rotation, which are important properties in the iris recognition. Third, to reduce the effect of extreme values in the feature matrix the extracted feature set was transformed and normalized, which remarkably improved the recognition rate. Fourth, mRMR was employed as a feature selector which has proven to be one of the most powerful and stable among known feature

selectors. Finally, to estimate the mean accuracy of the proposed method LOOCV was used. The obtained average accuracies on CASIA Ver.4 and Ver.1 were 96.55% and 98.29% respectively, and the accuracies without using LOOCV for both datasets were 100% which empirically illustrate the reliability and effectiveness of the presented method.

ACKNOWLEDGEMENTS

This work has been partially supported by the QREN funded project SLEEPTIGHT, with FEDER reference CENTRO-01-0202-FEDER-011530.

REFERENCES

- Aksoy, S., Haralick, R. M., 2001. Feature Normalization and Likelihood-Based Similarity Measures for Image Retrieval. *Pattern Recognition letters*. 22(2001), pp. 563-582.
- Becq, G., Charbonnier, S., Chapotot, F., Buguet, A., Bourdon, L., Baconnier, P., 2005. Comparison Between Five Classifiers for Automatic Scoring of Human Sleep Recordings. S.K. Halgamuge, L. Wang (Eds.), *Studies in Computational Intelligence (SCI)*, 4: Classification and Clustering for Knowledge Discovery. Springer-Verlag, pp. 113-127.
- Burges, J. C., 1998. A Tutorial on Support Vector Machines for Pattern Recognition. *Data Mining and Knowledge Discovery*. Vol. 2, pp. 121-167.
- CASIA Iris Image Database, <http://www.cbsr.ia.ac.cn/IrisDatabase.htm>.
- Chen, C. H., Chu, C. T., 2009. High Performance Iris Recognition Based on 1-D Circular Feature Extraction and PSO-PNN Classifier. *Expert Systems with Applications*. Vol. 36, No. 7, pp. 10351-10356.
- Clausi, D. A., 2002. An Analysis of Co-Occurrence Texture Statistics as a Function of Grey Level Quantization, *Can. J. Remote Sensing*. Vol. 28, No. 1, pp. 45-62.
- Cunha, A. L., Zhou, J., Do, M. N., 2006. The Nonsubsampled Contourlet Transform: Theory, Design, and Applications. *IEEE Trans. on Image Processing*. Vol. 15, No. 10, pp. 3089-3101.
- Daugman, J. G., 1993. High Confidence Visual Recognition of Personals by a Test of Statistical Independence. *IEEE Transactions on Pattern Analysis and Machine Intelligence*. Vol. 15, No. 11, pp. 1148-1160.
- Do, M. N., Vetterli, M., 2001. Pyramidal Directional Filter Banks and Curvelets. *IEEE Int. Conf. on Image Processing*. Vol. 3, pp. 158-161.
- Haralick, R. M., Shanmugam, K., Dinstein, I., 1973. Textural Features of Image Classification, *IEEE Transactions on Systems, Man and Cybernetics*. Vol. 3, No. 6.
- Li, M., Jiang, M., Han, M., Yang, M., 2010. Iris Recognition Based on a Novel Multi Resolution Analysis Framework. *IEEE 17th International Conference on Image Processing*, pp. 26-29.
- Masek, L., Kovesi, P., 2003. MATLAB Source Code for a Biometric Identification System Based on Iris Patterns. *The School of Computer Science and Software Engineering, the University of Western Australia*.
- Nonsubsampled Contourlet Toolbox <http://www.mathworks.com/matlabcentral/fileexchange/10049>
- Peng, H., Long, F., Ding, C., 2005. Feature Selection Based on Mutual Information: Criteria of Max-Dependency, Max-Relevance, and Min-Redundancy. *IEEE Transactions on Pattern Analysis and Machine Intelligence*. Vol. 27, No. 8, pp. 1226-1238.
- Po, D. D. Y., Do, M. N., 2006. Directional Multiscale Modeling of Images Using the Contourlet Transform. *IEEE Trans. on Image Processing*. Vol.15, Issue 6.
- Poursaberi, A., Araabi, B. N., 2007. Iris Recognition for Partially Occluded Images: Methodology and Sensitivity Analysis. *EURASIP Journal on applied Signal Processing*. Vol. 2007, Issue 1.
- Qi M., Lu Y., Li J., Li X., Kong T., 2008. User-Specific Iris Authentication Based on Feature Selection. *International Conference on Computer Science and Software Engineering*.
- Roy, K., Bhattacharya, P., Suen, C. Y., 2011. Towards Non Ideal Iris Recognition Based on Level Set Method, Genetic Algorithms and Adaptive Asymmetrical SVMs. *Engineering Applications of Artificial Intelligence*. Vol. 24, No. 3, pp. 458-475.
- Shah, S., Ross, A., 2009. Iris Segmentation Using Geodesic Active Contours. *IEEE Transactions on Information Forensics and Security*. Vol. 4, No. 4, pp. 824-836.
- Soh, L., Tsatsoulis, C., 1999. Texture Analysis of SAR Sea Ice Imagery Using Gray Level Co-Occurrence Matrices. *IEEE Transactions on Geoscience and Remote Sensing*. Vol. 37, No. 2.
- SVM and Kernel Method Toolbox, <http://asi.insarouen.fr/enseignants/~arakotom/toolbox/index.html>
- Wildes, R., 1997. Iris Recognition: An Emerging Biometric Tech. *Proc. IEEE*. Vol. 85, No. 9, pp. 1348-1363.